ACS Macro Letters

Letter

pubs.acs.org/macroletters

Charge Renormalization for Ellipsoidal Macroions

YongSeok Jho,*[,†,‡] Jonathan Landy,*[,§] and P. A. Pincus[∥]

[†]Asia-Pacific Center for Theoretical Physics, Pohang, Gyeongbuk 790-784, South Korea

[‡]Physics Department, POSTECH, Pohang, South Korea

[§]Chemistry Department, University of California, Berkeley, California, United States

[∥]Physics and Materials Departments, University of California, Santa Barbara, California, United States

Supporting Information

ABSTRACT: We study the problem of counterion condensation for ellipsoidal macroions, a geometry well-suited for modeling liquid crystals, anisotropic vesicles, and polymers. We find that the ions within an ellipsoid's condensation layer are relatively unrestricted in their motions, and consequently work to establish a quasi-equipotential at its surface. This simplifies the application of Alexander et al.'s procedure, enabling us to obtain accurate analytic estimates for the critical valence of a general ellipsoid in the weak screening limit. Interestingly, we find that the critical valence of an eccentric ellipsoid is always larger than that of the sphere of equal volume, implying that counterion condensation provides a force resisting the deformation of spherical macroions. This contrasts with a recent study of flexible spherical macroions, which observed a preference for deformation into flattened shapes when considering only linear effects. Our work suggests that the balance of these competing forces might alter the nature of the transition.

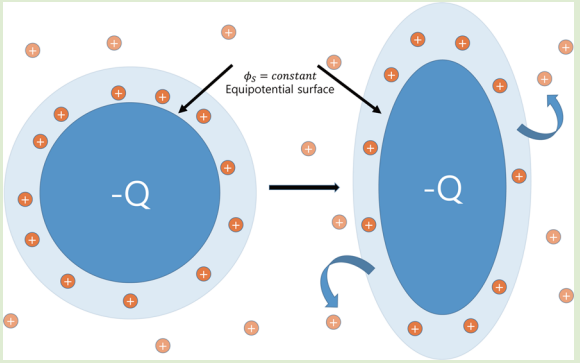

The behavior of weakly charged macroions in biological and soft materials is well described by the DLVO theory, which assumes very weak variations of the electrostatic potential, less than k_BT, over scales comparable to the screening length.[1] In this limit, the counterions (or salt ions) within one screening length of a macroion are not bound to its surface, but are free to move. This approximation breaks down near highly charged macroions, where the counterions are bound to the surface and form a condensation layer.[2] The distribution and behavior of the counterions within this layer are not well-characterized by mean field analysis. Instead, they are highly localized, and can be considered part of a macroion-condensed counterion composite, which moves about as a single entity.[2−7] Considering the averaged field of this composite, one can construct a generalized DLVO theory based on the effective, renormalized charge.[8−10]

The degree of charge renormalization depends upon the shape of a macroion. As explained by Zimm and Le Bret, in the zero salt concentration limit, no condensation occurs for an isolated spherical macroion, because the attractive energy gained through condensation onto such a macroion is always less than the entropy associated with ion liberation.[11] In contrast, a finite fraction and complete counterion condensation occurs for cylindrical and planar macroions, respectively, in the same limit.[12,13] Counterion condensation is expected for all geometries under finite salt concentration conditions.[4,14−19] The most drastic, qualitative change occurs for the spherical geometry, for which a finite fraction of counterions now condense. This was first explained by Alexander et al., who obtained the condensation fraction by simply requiring the surface potential to equate to the free ion entropy.[2] These behaviors are of interest in that various experimental measures relating to macromolecule solutions, including the osmotic pressure, structure factor, and compressibility vary with macroion effective charge.[8−10]

Studies on charge renormalization have largely focused on the symmetric geometries mentioned above because they are the most tractable. However, many physical systems of interest are not well-modeled by these idealized forms. Examples include charged liquid crystals, natural clay particles,[20,21] short polyelectrolyte chains and bundles,[22] and emulsions or vesicles of lipids characterized by high-anisotropy. The condensation characteristics of these intermediate geometries have not yet been mapped out. Further, these are not readily inferred from the symmetric geometry results, given the fact that these each differ qualitatively from one another. In this paper, we study the effective charge of a general ellipsoidal macroion in the low salt limit.

Quasi-equipotential development: Within the framework of condensation theory, the degree of counterion condensation is related to a macroion's surface potential.[2] Unfortunately, this value is often not uniquely defined for nonuniform geometries.

Received: April 20, 2015
Accepted: May 26, 2015
Published: May 29, 2015

DOI: 10.1021/acsmacrolett.5b00252
ACS Macro Lett. 2015, 4, 640−644

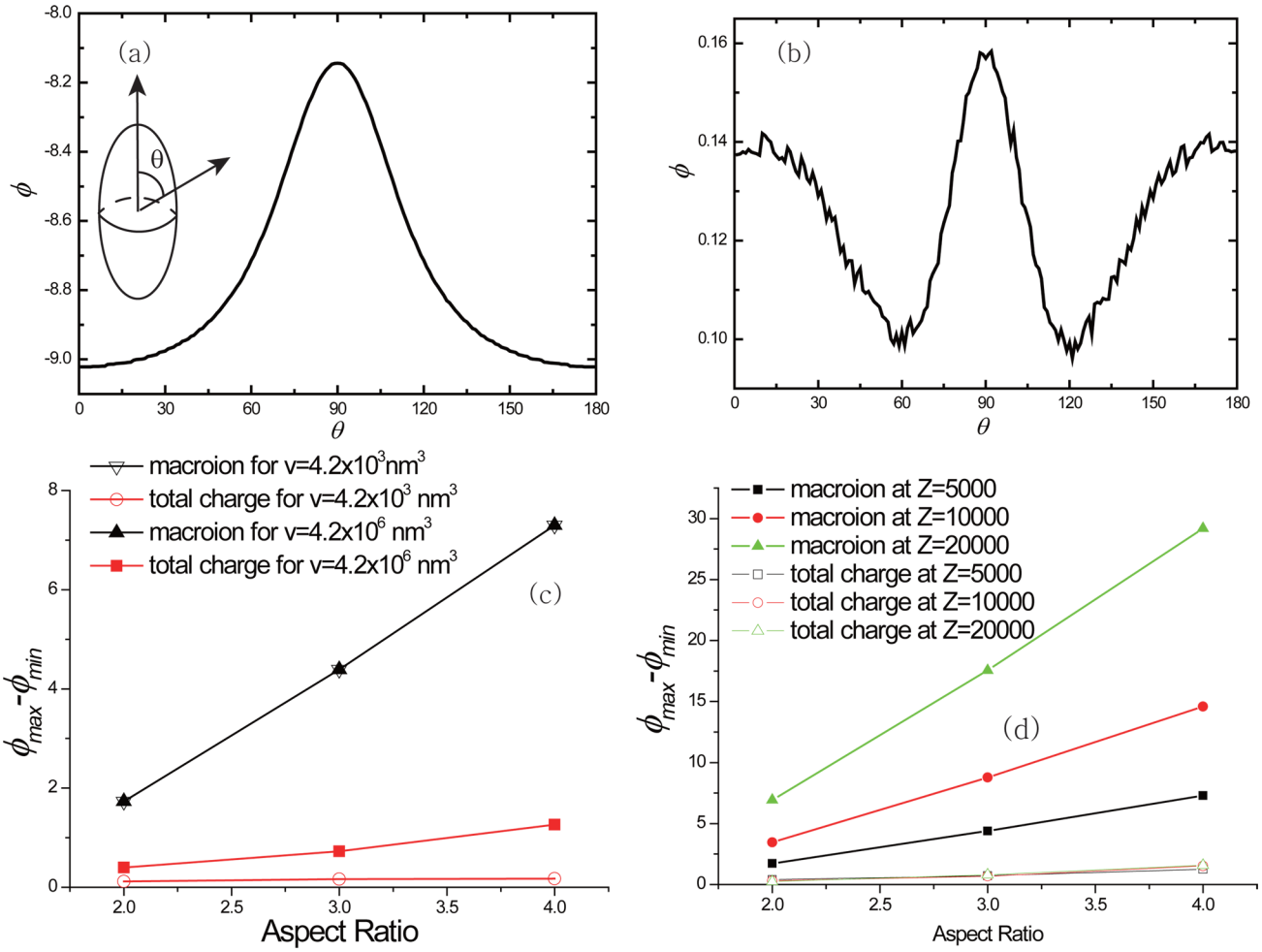

Figure 1. Potential (in k_BT) from the (a) prolate ellipsoidal macroion (aspect ratio 1:3) and (b) total charges are plotted as a function of polar angle, θ. (c, d) Maximum difference of potential of the total charges and that from the macroion are presented with respect to the aspect ratio. ϕ_v (volume fraction) is 0.01, and the volume of the ellipse is (c) $4\pi 10^3$ nm^3 (filled symbols) and $4\pi 100^3$ nm^3 (hollow symbols) when $Z = -5000e$. (d) Maximum potential difference of the macroion (filled symbols) and total charges (hollow symbols) for various macroion charge are plotted at volume $4\pi 100^3$ nm^3.

One condition where this complication is avoided is provided by the high salt limit:[3] In this case, all geometries basically resemble the planar case, because screening occurs locally, over length scales much smaller than those characterizing surface curvature. This argument is intuitive for $\kappa a \gg 1$, with κ the inverse Debye length and a the smallest macroion length scale, but Trizac et al. found that it actually holds reasonably well for all $\kappa a \gtrsim 1$.[3]

Here, we study ellipsoids in the $\kappa a \lesssim 1$ limit, where the locally planar approximation[3] does not hold. Nevertheless, we suggest that an equipotential surface can also develop in this limit, but for a different reason. In this case, at high bare macroion charge, significant counterion condensation occurs. At low ion density, these condensed ions will be strongly constrained in their motions along the surface normal direction, but relatively unrestricted in motions parallel to the surface. With sufficient mobile charge at the surface, the solution should resemble that for a conductor, resulting in a quasi-equipotential at the macroion surface.

To confirm that the ideas above hold, we have carried out various simulations of uniformly charged ellipsoids, screened by their counterions in the absence of salt. The simulations were run with the counterions constrained to sit within a spherical volume 100× larger than the ellipsoids, which were placed at the centers of these volumes. In Figure 1a,b, we plot two surface potential curves for one example counterion-screened ellipsoid as a function of the polar angle. The potential in (a) is that due to the bare charge ($-1000e$ total, a large value corresponding to a surface charge density of about -0.8 e/nm^2, guaranteeing significant condensation) of the macroion alone, while that in (b) is the total potential, which is the sum of the terms coming from the bare macroion and counterions combined. The potential from the bare surface is maximized at the equator and minimized at the poles. This maximum potential difference between these values is sizable, about $1k_BT$. In contrast, the maximum potential difference observed in the total surface potential plot is only about $0.05k_BT$, 20× smaller: The condensed ions have distributed themselves so as to nearly cancel out all potential variations at the surface, as expected. There is a small oscillation in potential variation which probably is associated with finite counterion size effects. The plots in Figure 1c,d demonstrate that these ideas hold quite generally. Here, we plot the maximum differences of the bare and total surface potentials against ellipsoid aspect ratio, at fixed volume, the volume is fixed to be that of a sphere of radius 10 and 100 nm in (c) and (d), respectively. We plot these results

DOI: 10.1021/acsmacrolett.5b00252
ACS Macro Lett. 2015, 4, 640−644

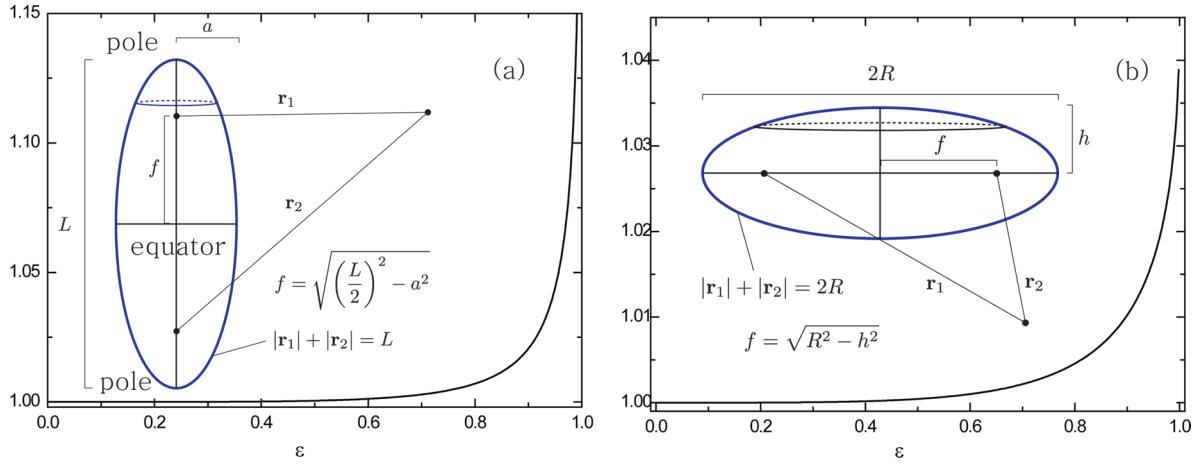

Figure 2. (a) Ratio of the exact prolate and spherical approximate potentials versus eccentricity. An example prolate ellipsoid of length L and radius a is presented in inset. (b) Ratio of 5 and 7 vs ϵ. An example oblate ellipsoid of radius R and height h is presented in inset.

for three different bare surface charge values. In all cases, the maximum difference is always significantly reduced in the total potential, relative to that of the bare potential. Further, this total maximum difference is never significantly larger than $1k_BT$, implying that the condensed ions are able to access the full surface through thermal excitations. In summary, we see that small potential variations can persist after counterion condensation has set in, but the variations are always weak relative to those associated with the bare surface charge.

Critical charge estimates: Having confirmed that counterion condensation results in a nearly uniform surface potential for highly charged ellipsoids, we now turn to the application of Alexander et al.'s procedure for estimating their critical valence. To estimate ellipsoid surface potentials, we will be making use of the Laplace approximation, equivalent to assuming no screening outside of condensation effects. This approximation will work well at small values of κa, since in this limit, the $1/r$ decay will significantly damp the potential of the macroion on scales shorter than the screening length. There are two cases to consider, prolate (extended) and oblate (flattened) ellipsoids.

Prolate ellipsoids: An example prolate ellipsoid is shown in inset of Figure 2a. The Laplacian separates in the coordinates (σ, τ, ϕ), where $|\mathbf{r}_1| + |\mathbf{r}_2| \equiv 2f\sigma$, $|\mathbf{r}_1| - |\mathbf{r}_2| \equiv 2f\tau$, and ϕ is the azimuthal angle; here, the $|\mathbf{r}_i|$ are the distances to the ellipsoid's focal points and f is its focal length (see figure). In these coordinates, the surface potential is

$$\phi = \frac{Q}{Da}\frac{\sqrt{1-\epsilon^2}}{2\epsilon}\log\left(\frac{1+\epsilon}{1-\epsilon}\right) \tag{1}$$

where $\epsilon \equiv ((2f)/(L))$ is the ellipsoid eccentricity (see Supporting Information (SI) for derivation). We note that the ellipsoid converges to the spherical limit as $\epsilon \to 0$. Setting the chemical potential of the free, z-valence counterions ($\mu = k_B T \log c$) equal to the potential of the ions bound to the surface, we obtain for the critical valence,

$$Z^* = -\frac{2\epsilon}{\sqrt{1-\epsilon^2}\,\log[(1+\epsilon)/(1-\epsilon)]} \times \frac{a}{zl_B}\log c \tag{2}$$

This equation is actually an implicit expression for Z^*, since c is a function of both Z^* and the volume of the cell in which the ellipsoid sits. We provide some numerical solutions to this equation below, and compare to critical valence values returned by simulations.

It is interesting to consider the limiting behaviors of 2. We consider first the nearly spherical limit: If the eccentricity is not too close to 1, it turns out that the potential 1 is nearly equal to that of a sphere charged to Q with radius given by the arithmetic mean of the three semiaxes of the ellipsoid, $\bar{a} \equiv (1/3)(a + a + L/2)$. That is,

$$\phi \approx \frac{Q}{D\bar{a}} = \frac{Q}{Da} \times \frac{3}{\left[2 + \left(1/\sqrt{1-\epsilon^2}\right)\right]} \tag{3}$$

With this approximation, the critical valence goes to

$$Z^* \approx -\frac{\bar{a}}{zl_B}\log c \tag{4}$$

This agrees formally with 2 only to order ϵ^2. Nevertheless, as shown in Figure 2a, eq 4 is within 1% error for all $\epsilon \lesssim 0.83$ and within 10% error for all values of $\epsilon \lesssim 0.98$. These values correspond to approximate aspect ratios of 2:1 and 5:1, respectively. As the aspect ratio goes above this value, their ratio raises sharply, diverging logarithmically in the $\epsilon \to 1$ limit. We discuss this elongated limit in the SI, where we show how to recover Manning's result for the critical valence of a line charge using eq 2.

Oblate ellipsoids: An oblate ellipsoid is one whose two largest semiaxes are equal in length. An example is shown in the inset of Figure 2b. A calculation similar to that used in the prolate case, but carried out in oblate spheroidal coordinates,[23] gives the following Laplace approximation to the surface potential

$$\phi = \frac{\sqrt{1-\epsilon^2}}{\epsilon}\tan^{-1}\left(\frac{\epsilon}{\sqrt{1-\epsilon^2}}\right) \times \frac{Q}{Dh} \tag{5}$$

The corresponding critical valence is

$$Z^* = -\frac{\epsilon}{\sqrt{1-\epsilon^2}\,\tan^{-1}\left(\epsilon/\sqrt{1-\epsilon^2}\right)} \times \frac{h}{zl_B}\log c \tag{6}$$

We now consider the spherical approximation to the oblate case, considering a sphere of charge Q and radius $\bar{h} \equiv (1/3)(2R + h)$. This approximates the surface potential as

$$\phi \approx \frac{Q}{D\bar{h}} \tag{7}$$

DOI: 10.1021/acsmacrolett.5b00252
ACS Macro Lett. 2015, 4, 640−644

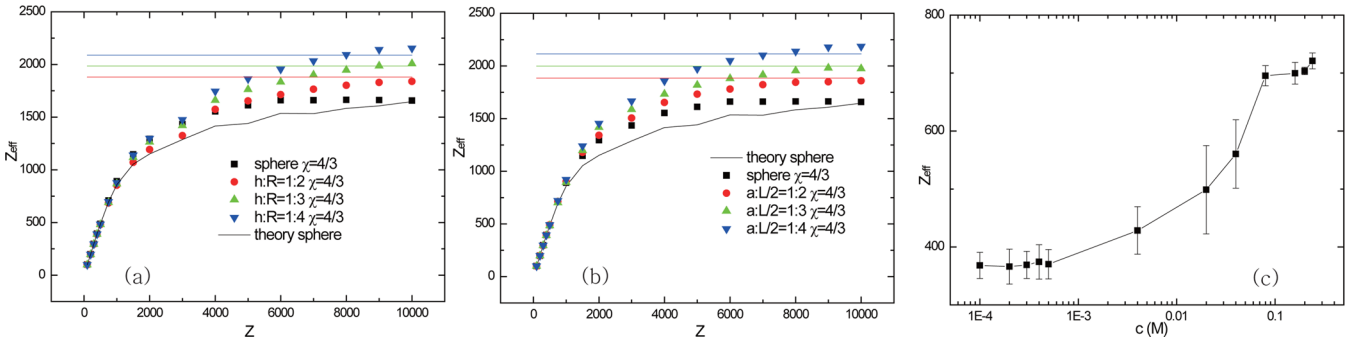

Figure 3. Effective charge of ellipsoidal macroions is presented. The lines "theory sphere" are obtained by the process in ref,[2] and points are from the numerical simulation. The aspect ratios of the ellipsoids are 1:1, 1:2, 1:3, and 1:4, respectively, for (a) oblate (b) prolate at $\phi_v = 0.001$. The volume of the ellipse is $(4\pi/3)(100)^3$ nm^3 (c) The salt concentration is varied; $\epsilon = 0.94$, $Z = 1000$, $\phi_v = 0.01$, and the volume is $(4\pi/3)(100)^3$ nm^3.

In Figure 2b, we plot the ratio of eqs 5 and 7. This peaks at a value of approximately 1.05 at $\epsilon = 1$, where the prefactors both approach zero. The plot shows that the spherical approximation works quite well for all ϵ given an oblate ellipsoid. We recover the familiar planar result in the limit $h \to 0$ (details in SI).

Comparison with numerical results: We now turn to simulation checks of the critical valence estimates derived in the previous sections (Methods are detailed in the SI). In Figure 3a,b, the effective charge of various oblate and prolate ellipsoids, screened by their counterions only, are displayed as a function of bare surface valence Z. The colored, horizontal lines shown are our Laplace approximation critical valence estimates, obtained by numerically solving eq 2. The points shown were obtained from our simulations using the Diehl method,[6] and the solid, black curve shown was obtained using the Alexander et al. procedure for a spherical macroion. Their consistency confirms that the condensation fraction is fairly well-defined, and that numerical estimates of this quantity are largely insensitive to which particular procedure is used. At large valence, Z_{eff} appears to converge to a limiting value, Z^* (to be precise, it must continue to vary weakly, logarithmically, with Z). The limiting Z^* values agree very well with our analytic estimates, confirming the accuracy of the equipotential/Laplace approximation approach.

Interestingly, Z_{eff} is almost independent of aspect ratio until $Z \simeq 2000$ e. At higher valence, Z_{eff} grows with ellipsoid aspect ratio. In other words, fewer ions condense for more asymmetric ellipsoids. This is easily understood given the results of the previous sections, where we found that the spherical approximation works well for ellipsoids of low to moderate eccentricity: In these limits, the critical valence of an ellipsoid is linearly proportional to its mean-axial length, a value that increases with eccentricity when its volume is held fixed (for intuition, consider the arithmetic-geometric mean inequality). It is important to point out that these observations do not contradict known Zimm and Le Bret behavior results, which predict zero condensation for charged spheres, but fractional and full condensation for charged cylinders and planes, respectively. The reason is that the plots shown here are in terms of Z: At fixed Z, both elongated planes and cylinders end up having zero charge density, and so no condensate. This is explicit in Manning's formula for the cylindrical case. For planes, this follows from (6) of the SI.

It is interesting to relate the observations above to the stability of a highly charged spherical macroion. As we have seen, if a spherical macroion is deformed into an eccentric ellipsoidal geometry of equal volume, its critical valence will increase. The release of counterions will generate an effective force that serves to stabilize the spherical geometry: A counterion will bind to a macroion only when its electrostatic energy benefit exceeds its entropy loss. Thus, a reduction in condensation implies a net increase in the free energy of the ions released. Interestingly, a recent simulation study has found that other electrostatic effects can drive a flexible charged macroion through a shape transition at low salt, away from the spherical geometry and into a dimpled shape, similar to those of blood cells.[24] It would be interesting to consider extending this prior analysis to see whether the inclusion of condensation effects can significantly modify the nature of the transition.

In Figure 3c, we present simulation results relating to the dependence of an ellipsoid's critical valence on added monovalent salt concentration. At low c and large V, it must increase, as one transitions from Zimm-Lebret to finite c behavior. However, as we see here, at finite volumes, Z^* increases with c. The reason is that a larger salt concentration results in a shorter Debye length. Because of this, the surface potential is reduced, lessening the driving force for condensation and, also, simultaneously weakening the interaction between macroions, as one would generally expect.

Discussion: We have found that the counterions in the condensation layer generate a quasi-equipotential surface near highly charged macroions. Here, we exploited this observation, combining the equipotential surface approximation with the Alexander et al. procedure to obtain accurate estimates for a general ellipsoid's critical valence. Interestingly, we found that the spherical result often provides a good approximation, with spherical radius set to the ellipsoid's mean semiaxial length. This implies that counterion condensation should decrease when a spherical macroion is deformed to other shapes of equal volume, providing a stabilizing force for the spherical geometry.

It would be a simple matter to extend the results derived here to the moderate salt regime, where the screening length becomes comparable to the macromolecule's size. In this case, one need only apply the Debye−Hückel approximation to estimate surface potentials, rather than the Laplace approximation, which we have made use of here for simplicity's sake. Series expansions to the Debye−Hückel equation exists for ellipsoidal, constant surface potential geometries.[25] It would also be interesting to study whether the quasi-equipotential approximation holds for more general geometries.

DOI: 10.1021/acsmacrolett.5b00252
ACS Macro Lett. 2015, 4, 640−644

■ ASSOCIATED CONTENT

Supporting Information

The detail of Laplace equation, limiting case studies of the solution, and numerical details. The Supporting Information is available free of charge on the ACS Publications website at DOI: 10.1021/acsmacrolett.5b00252.

■ AUTHOR INFORMATION

Corresponding Authors

*E-mail: ysjho@apctp.org.
*E-mail: jslandy@gmail.com.

Notes

The authors declare no competing financial interest.

■ REFERENCES

(1) Verwey, E. J. W.; Overbeek, J. T. G.; Overbeek, J. T. G. *Theory of the Stability of Lyophobic Colloids*; Courier Corporation: Chelmsford, MA, 1999.
(2) Alexander, S.; Chaikin, P.; Grant, P.; Morales, G.; Pincus, P.; Hone, D. *J. Chem. Phys.* **1984**, *80*, 5776−5781.
(3) Trizac, E.; Bocquet, L.; Aubouy, M. *Phys. Rev. Lett.* **2002**, *89*, 248301.
(4) Manning, G. S. *J. Phys. Chem. B* **2007**, *111*, 8554−8559.
(5) Manning, G. S. *Biophys. Chem.* **2002**, *101*, 461−473.
(6) Diehl, A.; Levin, Y. *J. Chem. Phys.* **2004**, *121*, 12100−12103.
(7) Borukhov, I. *J. Polym. Sci., Part B: Polym. Phys.* **2004**, *42*, 3598−3615.
(8) Monovoukas, Y.; Gast, A. P. *J. Colloid Interface Sci.* **1989**, *128*, 533−548.
(9) Mitaku, S.; Ohtsuki, T.; Enari, K.; Kishimoto, A.; Okano, K. *Jpn. J. Appl. Phys.* **1978**, *17*, 305.
(10) Lindsay, H.; Chaikin, P. *J. Chem. Phys.* **1982**, *76*, 3774−3781.
(11) Zimm, B. H.; Bret, M. L. *J. Biomol. Struct. Dyn.* **1983**, *1*, 461−471.
(12) Oosawa, F. *Polyelectrolytes*; Marcel Dekker: New York, 1971.
(13) Manning, G. S. *J. Chem. Phys.* **1969**, *51*, 924−933.
(14) Stern, O. Z. *Elektrochem.* **1924**, *30*, 508.
(15) Henle, M. L.; Santangelo, C. D.; Patel, D. M.; Pincus, P. A. *Europhys. Lett.* **2004**, *66*, 284.
(16) Wong, G. C.; Lin, A.; Tang, J. X.; Li, Y.; Janmey, P. A.; Safinya, C. R. *Phys. Rev. Lett.* **2003**, *91*, 018103.
(17) Wen, Q.; Tang, J. X. *J. Chem. Phys.* **2004**, *121*, 12666−12670.
(18) Landy, J.; McIntosh, D. B.; Saleh, O. A. *Phys. Rev. Lett.* **2012**, *109*, 048301.
(19) Landy, J.; Lee, Y.; Jho, Y. *Phys. Rev. E* **2013**, *88*, 052315.
(20) Davidson, P.; Gabriel, J.-C. P. *Curr. Opin. Colloid Interface Sci.* **2005**, *9*, 377−383.
(21) Dijkstra, M.; Hansen, J.; Madden, P. *Phys. Rev. Lett.* **1995**, *75*, 2236.
(22) Radeva, T. *Colloids Surf., A* **2002**, *209*, 219−225.
(23) Arfken, G. B. *Mathematical Methods for Physicists*, 4th ed.; Academic Press: New York, 1970.
(24) Jadhao, V.; Thomas, C. K.; de la Cruz, M. O. *Proc. Natl. Acad. Sci. U.S.A.* **2014**, *111*, 12673−12678.
(25) Álvarez, C.; Téllez, G. *J. Chem. Phys.* **2010**, *133*, 144908.

DOI: 10.1021/acsmacrolett.5b00252
ACS Macro Lett. 2015, 4, 640−644